European Polymer Journal 185 (2023) 111804

Contents lists available at ScienceDirect

European Polymer Journal

journal homepage: www.elsevier.com/locate/europolj

Environmentally friendly, antibacterial materials from recycled keratin incorporated electrospun PLA films with tunable properties

Dicle Ayca Ertek [a], Nazmiye Ozlem Sanli [b], Yusuf Ziya Menceloglu [c,d], Senem Avaz Seven [c,e,*]

[a] Marmara University, Faculty of Technology, Textile Engineering, 34722 Istanbul, Turkey
[b] Istanbul University, Department of Biology, Faculty of Science, 34418 Istanbul, Turkey
[c] Sabanci University, Faculty of Engineering and Natural Sciences, 34956 Istanbul, Turkey
[d] Sabanci University Integrated Manufacturing Technologies Research and Application Center & Composite Technologies Center of Excellence, Teknopark, 34906 Istanbul, Turkey
[e] Bahcesehir University, Faculty of Engineering and Natural Sciences, Yildiz, Çiragan Cd., 34349 Istanbul Turkey

ARTICLE INFO

Keywords:
Keratin electrospinning
Recycled keratin
Poultry waste
Antibacterial packaging

ABSTRACT

The traditional disposal of chicken feathers includes expensive and challenging steps such as incineration and burying in landfills. Keratin is a valuable component of chicken feather waste recycled from poultry industry. The fibrous intermediate protein nature along with unique chemical composition enables its use in food, pharmaceutical, cosmetics and agricultural industries. The current study proposes an innovative valorization of recycled keratin from chicken feathers combined with polylactic acid (PLA), a viable bio-based polymer obtained from plant-based food stock. As a novel application, this study explains the preparation, electrospinning parameter optimization and performance assessment of recycled keratin electrospun with PLA. The structural, thermal, thermo-mechanical, morphological, antibacterial and surface wetting properties of keratin-incorporated electrospun PLA films were investigated. The disruption of crystallinity, hence the processability of both biopolymer via electrospinning is demonstrated. The nanofiber size, thermal, thermo-mechanical, antibacterial and surface wetting properties of electrospun films can be tuned by keratin content. This study provides environmentally friendly, recycled, bio-based material alternatives with tunable material properties that can be used in multitude of applications including environmental food packaging.

1. Introduction

The use of natural polymers as a component of sustainable industrial materials is a developing research field to replace the non-biodegradable synthetic plastics. Keratin is one of the most abundant animal sourced biopolymer and a major side product of poultry industry. It is extracted from several sources including wool [1], human hair [2], chicken feathers [3,4], sole fish skin [5] and many others [6] using well established methods of oxidation [7], reduction [8], ionic liquid immersion [9], steam explosion [10]. Although the fibrous, cysteine-rich nature present wide variety of properties, β-keratin is the primary type of keratin in feathers [11]. This form of keratin is characterized by dominant β-sheets and plates whereas the α- form is rich in α-helices. The abundance of disulfide bonds gives a high conformational stability to keratin protein.

Keratins have been attractive biomaterial research subject or more than three decades [12] due to their ability to form loosely packed filaments that provide resilience to tissues [11]. Therefore, there are several literature examples on the use of keratin as biomaterial for tissue engineering in the form of scaffolds [13–15], films [16–18] and microcapsules [19]. In addition to that, electrospun keratin-based films and mats are also another important study subject in biomaterials [20] as well as packaging [21–23].

As an efficient way of non-woven nano-sized fiber generation, electrospinning has shown promising potential in many applications including antibacterial active packaging. There has been attempts to perform electrospinning of keratin without using a carrier polymer [24]. But relatively poor viscoelastic properties of natural macromolecules, along with their brittleness makes them a poor candidate for electrospinning applications [25]. For this reason, keratin is a challenging material to electrospin alone [20,25]. Nevertheless, good solvents for proteins that enables the disruption of intra- and inter-molecular

* Corresponding author.
E-mail address: senem.seven@eng.bau.edu.tr (S. Avaz Seven).

https://doi.org/10.1016/j.eurpolymj.2022.111804
Received 24 October 2022; Received in revised form 21 December 2022; Accepted 27 December 2022
Available online 30 December 2022

interactions in 3D protein conformation [26]. Other approach is to employ well-spinnable carrier polymers such as polyethylene oxide (PEO) [27], polyvinyl alcohol (PVA) [28], PLA [29], polyacrylonitrile PAN [30], chitosan [31] and silk fibroin [32] to solve this issue. In that sense, poly(l-lactic acid) PLA is a new generation sustainable polymer that is likely to replace petroleum-based industrial polymers. It's biodegradability and biocompatibility bring PLA important application fields in large industrial sectors such as agriculture [33] and food packaging [34]. In addition, wool keratins have shown to enhance the affinity of PLA [29].

The current study covers the design, development and performance enhancement of keratin-PLA based electrospun packaging materials with tunable material properties. The electrospun Ker-PLA mats have been assessed in terms of their structural, thermal, morphological, thermomechanical, antibacterial and surface properties. Throughout the study, the effect of two main parameters, *i.e.,* nanofiber formation by electrospinning process and the addition of keratin on the performance of PLA were investigated. For the ease of comparison, only one electrospun sample (50 wt% electrospun keratin containing electrospun PLA; KerPLA5/5-ES) was used in structural and thermal analyses. This was solely done to investigate the effect of keratin fiber formation and to exclude to fiber content effect. After that, the effect of keratin nanofiber content of morphological, thermomechanical, antibacterial and surface wetting properties were investigated with respect to increased keratin content in electrospun samples. The results, in general, put forth that electrospun Ker-PLA mats/films are useful as antibacterial environmentally friendly packaging materials.

2. Materials methods

2.1. Preparation of Keratin/polymer solutions

Recycled from chicken feather waste, extracted keratin (MW > 10 kDa) was provided by Consorzio Santacroce sull'Arno (SGS, Italy). In their novel keratin extraction method, keratin is hydrolyzed from chicken feathers by alkaline hydrolysis to obtain a final brix concentration of 35° [20]. Poly-Lactic Acid biopolymer granules that are in 3 mm nominal granule size (mentioned as PLA henceforth) was obtained from Sigma-Aldrich and used as is.

Keratin/polymer solutions were prepared in 1,1,1,3,3,3-Hexafluoro-2-propanol (HFIP) and acetone/chloroform (Ac/Chl) 7:3 v/v) solutions/mixtures at varying concentrations (10–20 % wt% keratin + polymer concentration) where keratin/polymer mixture ranges between 10:90 to 90:10 (m/m) by dissolving keratin and polymer (Gelatin Type A, PEG4000, PLA) separately under continuous stirring at room temperature (overnight) and finally mixing the polymer and keratin solutions.

2.2. Preparation of keratin based electrospun films

Factors affecting electrospinning parameters, such as applied voltage, solution flow rate, distance between needle tip and collector, solution concentration and solvent were screened. In the meantime, it is known that the polymer molecular weight is not the sole but a significant factor affecting the fiber diameter in electrospun fibers. The fiber diameter increases as the molecular weight of the polymer gets higher [35]. But as the molecular weight of extracted keratin is bound to the extraction process, the effect of molecular weight on electrospinning is not added as a parameter into the screening process. Once the parameters were set, the electrospun polymer fibers were collected on an aluminum foil. To determine the success of electrospinning, 4 criteria were evaluated; Taylor cone formation [36], jet continuity, bead-fiber ratio, fiber radius. The Taylor cone formation is an indicator showing that polymer jet is moving through the electric field. Jet continuity indicates the uniformity of polymer fibers collected on grounded collector. Taylor cone formation, along with jet continuity demonstrates the electric field applied overcomes the surface tension of polymer droplet. On the other hand, bead-fiber ratio and fiber radius are indicators of the success of electrospinning optimization process. Here, presence of bead and ribbon-like formations suggest insufficient volatility of carrier solvent which prevents polymer chains to expand during their flight between needle tip and collector (Figure S-1-a). Non-uniform fiber diameter is also an indicator of insufficient solvent flow rate and environmental factors.

Electrospinning process optimization were performed as described in Figure S-1-b. First, polymer solutions prepared in appropriate solvents were subjected to various electric fields and Taylor cone formation was monitored. The needle tip to collector distance and the lowest electric field value where the Taylor cone formation was observed determined the first step in Figure S-1-b. This was followed by the adjustment of polymer flow rate and needle-to-collector distance. Table 1 gives the details of all performed electrospinning procedures.

2.3. Preparation of keratin cast-films

Keratin based cast films were prepared to compare and evaluate the effect of electrospinning on material properties. Control film samples were prepared by casting electrospinning solutions into Teflon mold and oven-dried at 70 °C overnight.

2.4. FTIR

Prior to Fourier Transformed Infrared Spectroscopy (FTIR) analysis, all samples were dried at 70 °C in a vacuum oven to prevent the overlapping with water absorption band (1650 cm^{-1}) [37]. Attenuated Total Reflectance - Fourier Transformed Infrared (ATR-FTIR) spectra were collected on a Nicolet iS10 smart iTR spectrometer (Diamond) between 550 and 4000 cm^{-1} using a resolution of 0.5 cm^{-1}. Spectra were averaged from 32 scans and baseline corrected.

2.5. TGA

Thermal stabilities of Keratin based materials are determined by Thermogravimetry (TGA). This method measures the weight loss due to the formation of volatile species with respect to temperature rise. 20 mg keratin and PLA films, Ker-PLA cast and electrospun films were weighed and placed in TGA (Netzsch STA 449 F3) cruicibles and heated under nitrogen atmosphere (85 mL/min flow rate) between 25 and 1000 °C, with a heating rate of 10 °C/min.

2.6. DSC

Thermal properties of samples were analyzed using a Differential Scanning Calorimetry (DSC, TA Instruments, TA2000). Samples were subjected to a one cycle heat treatment without pre-heat treatment, starting from 25 °C, ramping with a rate of 10 °C/min, until 300 °C, in nitrogen atmosphere. DSC data were recorded in the first heating cycle.

2.7. SEM

Scanning Electron Microscopy (SEM) is used to monitor the morphology of keratin-based materials. Prior to SEM analysis sample surfaces were coated with a Pt/Pd thin layer. Secondary electron (SE) and InLens detectors were used to acquire images with varying gun voltages between 2 and 5 kV.

2.8. DMA

Dynamic Mechanical Analyses (DMA) were performed on a Metler Toledo DMA in tensile mode using a 1 Hz frequency with an amplitude of 5 μm while heated between 30 and 120 °C with a heating rate of 3 °C/min. Max heating temperature was adjusted with respect to sample decomposition dynamics. ASTM E 1640–13 standard was applied in

Table 1
Electrospinning parameter optimization results of keratin-based materials.

Sample Code	Sample (Ker-polymer ratio m/m, total Ker + polymer amount in solution wt%)	Solvent	Flow rate	Voltage (kV)	Distance (cm)	General Look/ Morphology
KerPLA9/1-ES	Ker-PLA (90/10, 10%)	Ac/Chl	0.01 mL/min	20	15	No electrospin
KerPLA7/3-ES	Ker-PLA (70/30, 10%)	Ac/Chl	0.01 mL/min	20	15	No electrospin
KerPLA5/5-ES	Ker-PLA (50/50, 10%)	Ac/Chl	0.01 mL/min	20	15	No electrospin
KerPLA3/7-ES	Ker-PLA (30/70, 10%)	Ac/Chl	0.01 mL/min	20	15	Bead
KerPLA1/9-ES	Ker-PLA (10/90, 10%)	Ac/Chl	0.01 mL/min	20	15	Bead
KerPLA7/3-ES	Ker-PLA (70/30%, 15%)	HFIP	0.01 mL/min	15 kV	15	No electrospin
KerPLA7/3-ES	Ker-PLA (70/30%, 15%)	HFIP	0.1 mL/h	15 kV	15	Bead
KerPLA5/5-ES	Ker-PLA (50/50%, 15%)	HFIP	0.1 mL/h	15 kV	15	Bead
KerPLA3/7-ES	Ker-PLA (30/70%, 15%)	HFIP	0.1 mL/h	15 kV	15	Bead-fiber
KerPLA3/7-ES	Ker-PLA (30/70%, 15%)	HFIP	0.1 mL/h	12 kV	15	Electrospun fiber
KerPLA5/5-ES	Ker-PLA (50/50%, 15%)	HFIP	0.1 mL/h	12 kV	15	Electrospun fiber
KerPLA7/3-ES	Ker-PLA (70/30%, 15%)	HFIP	0.1 mL/h	12 kV	15	Electrospun fiber
PLA-ES	PLA (15%)	HFIP	0.1 mL/h	12 kV	15	Electrospun fiber

specimen preparation.

2.9. Contact angle measurement

Contact angles of the keratin containing electrospun and film samples were measured by sessile drop method via a horizontally placed microscope attached to a camera. Contact angle measurements were performed on dried samples. The results were recorded as the average of five different measurements from different locations of sample surfaces.

2.10. Antibacterial activity

Antibacterial activity tests were performed at Istanbul University Faculty of Science, Biocidal Products and Microbial Technology Laboratory. Antibacterial activity of samples except Ker-F sample was evaluated by using Japanese Industrial Standard (JIS) Z 2801 (ISO 22196) test method. In antibacterial tests, *Staphylococcus aureus* ATCC 6538 and *Escherichia coli* ATCC 25,922 were employed as Gram-negative and Gram-positive bacteria, respectively.

(a) Japanese Industrial Standard Z 2801Test Method

According to the standard treated and untreated samples were cut into a square of 50 mm ± 2 mm. Samples were cleaned by using absorbent gauze pads immersed in ethanol 2 or 3 times and dried. 0.4 mL of diluted test bacteria in 1/500 Nutrient Broth (Oxoid) (2.5 to 10 × 105 cells/ml) were inoculated onto the each sample. After inoculation samples were covered with sterile film and incubated at 37 °C and a relative humidity of not <90 % for 24 h. At the end of contact time samples were transferred into the SCDLP broth (neutralizing medium) and homogenized by using stomacher. Diluted and undiluted homogenized samples were inoculated onto plate count agar (PCA, Oxoid) at 35 °C ± 1 °C for 40 h to 48 h. At the end of incubation, the number of colonies were counted. Bacteria reduction (%) was calculated using the following formula:

$$R = U_t - A_t$$

where R denotes the antibacterial activity, U_t and A_t are the logarithmic cell counts (kob/cm^2) of control and test samples, respectively. An R value > 2 is accounted as antibacterial.

(b) ASTM E2149 Standard Test Method

ASTM E2149 standard was followed to evaluate the antibacterial activity of Ker-F sample in dynamical contact conditions. Untreated and treated Ker-F samples were weighed to 1.0 ± 0.1 g. 50 mL bacterial inoculums were prepared a final concentration of 1.5–3.0 × 105 CFU/mL (colony forming unit/ml) for each treated and untreated specimen and added to sterile 250 mL screw-cap Erlenmeyer flasks. The series of flasks were incubated at 37 °C on the wrist-action shaker for 24 h. at the end of incubation, samples were neutralized by using polysorbate 80 and Lecithin broth media, then serially diluted and plated out in triplicate. Petri dishes were incubated at 35 °C ± 2 °C for 24 h to 48. Survived colonies were counted and values were converted CFU/ml and percent reduction of bacteria calculated using following formula:

$$R = \frac{(C - A)}{C} x100$$

where R is % reduction, A is the number of bacteria recovered from the inoculated treated test samples incubated for 24 h and C is the number of bacteria recovered from the inoculated untreated test samples after 24 h.

3. Results

3.1. Electrospinning process

Electrospinning process was followed as described in section Materials and Methods section. Among the various samples containing different weight ratio of polymers and/or dissolved in varying solvents (including 1:1 acetone chloroform mixture; Ac/Chl, and hexafluoro-2-propanol; HFIP). 13 sample were successfully collected on collector plate of the electrospinning setup. Those samples are listed in Table 1. The final morphologies of the prepared samples were investigated by Scanning Electron Microscopy. Among these 13, smooth electrospun nanofiber formations were only observed in the final 4 samples, where keratin was blended with PLA at varying weight ratios, dissolved in HFIP, placed in a syringe at 15 cm from the collector, and injected at a

rate of 0.1 mL/h under 12 kV voltage. These samples, along with the cast films were used for further analyses.

3.2. Structural characterization

FTIR spectroscopy is used in identifying the structural characteristics of Keratin-based electrospun films in different polymeric matrices and/or prepared by various processing techniques. The most prominent FTIR bands of keratin are amide I and amide II stretchings observed around 1620 and 1650 cm^{-1}, respectively. The absorption band at 1633 cm^{-1} characterizes the crystallization mode of β-sheets, while a shift in this band to 1650 cm^{-1} region reveals α-helix/coil formations [38,39]. Comparing FTIR spectra of Keratin-PLA (electrospun) samples with Keratin and PLA films', characteristic FTIR bands of both materials can easily be identified. The bands observed at 2996 cm^{-1} and 1749 cm^{-1} correspond to —C—H and —C═O stretchings of PLA, respectively. The shouldered band observed around 1179 cm^{-1} arises from the stretching vibrations of —O—C═ and —C—O groups [40]. A shift in 1749 cm^{-1} band observed in PLA to higher wavenumbers (1754 cm^{-1}, peak fitting details provided in Figure S-2) in electrospun Ker-PLA film designates a weakening in —C═O band (Fig. 1-a) [41]. This shows that secondary interactions formed between keratin and PLA during electrospinning dominates over —C═O bond strength. On the contrary, 1749 cm^{-1} band shift to lower values (1743 cm^{-1}) in Keratin-PLA cast film samples, implying fewer secondary interactions are formed after cast film process. In addition to —C═O region, one of the most prominent keratin bands of amide I characterized at 1639 cm^{-1} in keratin film samples (Fig. 1-b) is observed to shift to higher values (1650 and 1651 cm^{-1} for KerPLA-F and KerPLA-ES, respectively). In Keratin-PLA electrospun and cast films, this shift implies an increase in α-helix formations [42], hence an increase in crystallinity. Accordingly, it is concluded from FTIR spectra that PLA alters crystallinity of keratin, making significant changes in keratin's crystallinity and/or its folding mechanism.

3.3. Thermal properties

3.3.1. TGA

Fig. 2-a shows the thermogravimetry results of keratin film. Ker-F sample exhibit three weight loss phases [43–45]. The first phase is observed around 99 °C (8.39 %) is attributed to water content of keratin while the second phase is related with fiber decomposition of keratin with an onset of 226 °C (8.18 %). Third region is observed at 317 °C onset (50.93 %) corresponds to full protein denaturation (Fig. 2-a). A 16.07 % residue after complete degradation at 1000 °C relates with inorganic content of the protein. Fig. 2-b shows thermograms of PLA-F, PLA-ES, KerPLA-F and KerPLA-ES samples. Comparing PLA-F to PLA-ES, one can easily observe that the water content of PLA films decreases along with the thermal stabilities after electrospinning. This can be attributed to poor relaxation in polymer's conformation due to rapid solvent evaporation during electrospinning. In addition to this, incorporation of PLA significantly enhances thermal stability of keratin film, shifting thermal degradation onset temperatures from 317 °C to 346 °C (Fig. 2-a and -b). Same applies to electrospun sample (Fig. 2-b green); the onset temperature of degradation enhances up to 325 °C, but this increase is not as sharp as PLA incorporated film sample (Fig. 2-b magenta). Therefore, it is convenient to say that incorporation of PLA promotes thermally more stable films, but electrospinning lowers thermal stability. Here, it should be noted that the resemblance of thermal behavior of Ker-PLA samples is because of the higher PLA content in analyzed blends (KERPLA3/7-F and KERPLA3/7-ES).

Comparing the thermograms of KerPLA-F to KerPLA-ES, the sharp weight loss in KerPLA-F up to 200 °C distinguishes water and fiber content of protein. This means that water and fiber is more preserved in film form but in this measurement, it is not clear which one is the actual driving force behind this weight loss. DSC analysis will explain this behavior in more detail.

3.3.2. DSC

DSC results of KerPLA samples are displayed in Fig. 3. In Ker-F (Fig. 3, black), first broad endohermic peak corresponds to loss of protein water content (105 °C). In keratin samples, the endothermic events between 200 and 350 are usually attributed to protein denaturation followed by protein degradation [46]. The energy spent from 155 °C to 205 °C in the DSC analysis is associated with melting of α form crystallites from keratins in different moisture contents [47]. Endothermic peak > 250 °C relates with crystalline melting of the nanofibers and the area of this peak denotes total crystallinity [48,49]. Comparing PLA-F and PLA-ES samples, it is observed that both have similar T_m, ΔH_m, ΔH_d values but PLA-ES has lower T_d (329 °C) than PLA-F (345 °C). Comparing Keratin added PLA samples, it is first noticed that the degradation temperature lowers (T_d) with respect to keratin content. This is well correlated with TGA results from PLA point of view, as the incorporation of keratin lowers the thermal stability of PLA. The shift in PLA's T_d in KerPLA-F and KerPLA-ES samples highlights the presence of keratin and the interaction of polymer with protein subunits [50].

A broadening in the melting curve of PLA around 170 °C suggests more amorphous characteristics and loss of fiber structures which is observed in KerPLA-F sample. In addition, the melting enthalpy of

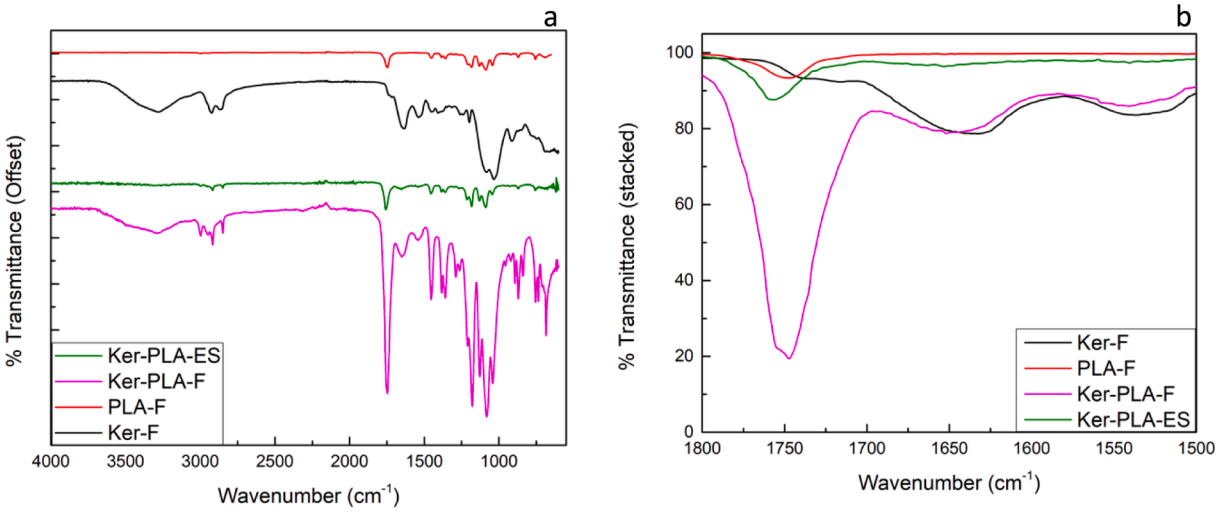

Fig. 1. Overall (a) and zoomed (b) FTIR spectra of keratin film (black), PLA (red), Ker-PLA cast film (magenta) and Ker-PLA electrospun film (green). (For interpretation of the references to colour in this figure legend, the reader is referred to the web version of this article.)

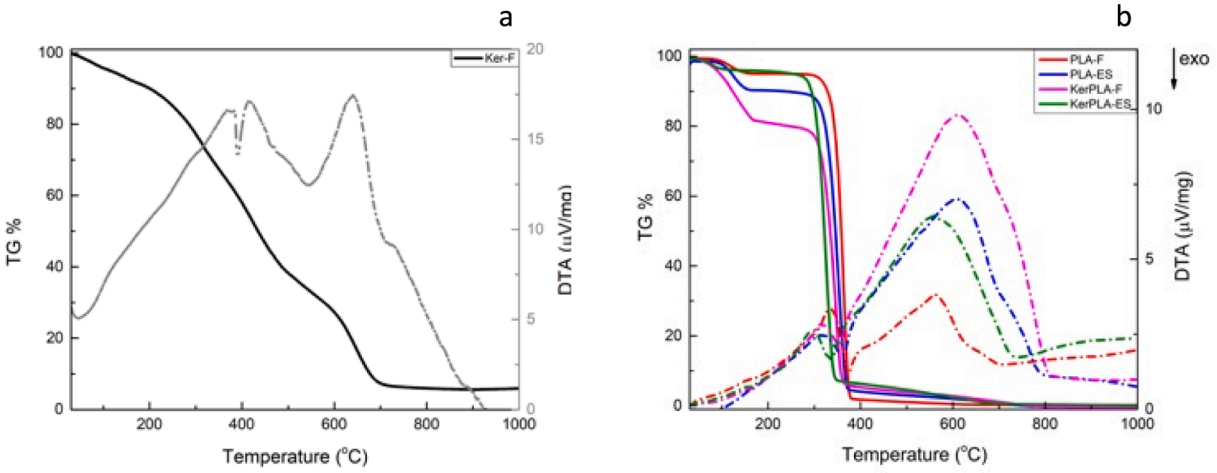

Fig. 2. TGA analysis of Ker-F (a), PLA-F (b, red), PLA-ES (b-blue), KerPLA-F (b, magenta) and KerPLA-ES (b, green). DTA curves are given in dash-dot representation. (For interpretation of the references to colour in this figure legend, the reader is referred to the web version of this article.)

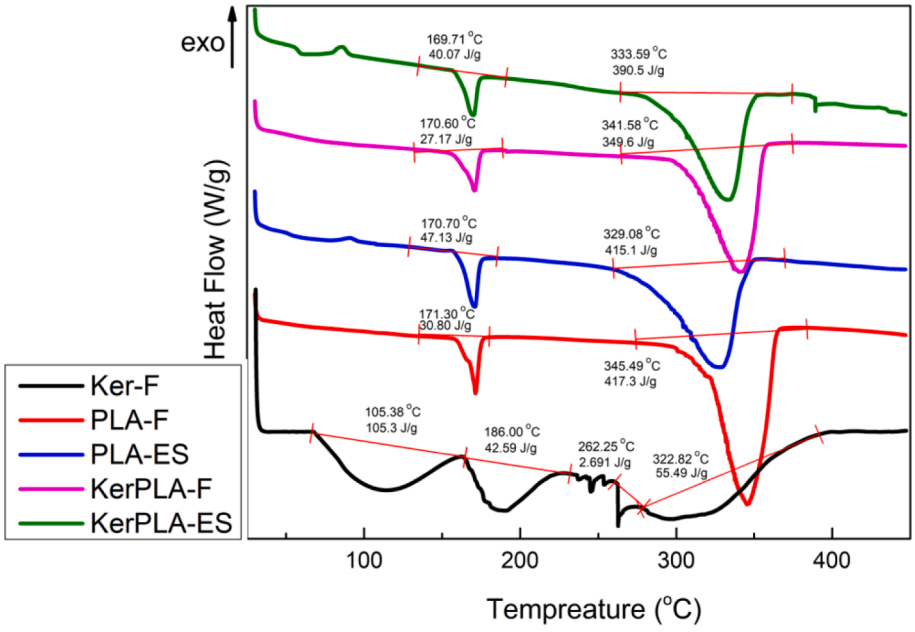

Fig. 3. DSC analysis of Ker-F (black), PLA-F (red), PLA-ES (blue), KerPLA-F (magenta) and KerPLA-ES (green). (For interpretation of the references to colour in this figure legend, the reader is referred to the web version of this article.)

KerPLA-F (27.27 J/g) is smaller than that of Ker-PLA-ES (40.07 J/g), suggesting that more fiber content is preserved in electrospun form. This completes the finding of more water and fiber content observed in TGA analysis of KerPLA-F and explains that the main driving force behind sharp weight loss in Fig. 2-b (magenta) is the water content of protein preserved in KerPLA-F sample. The presence keratin interferes with the mobility of PLA chains, favoring the formation of slightly less ordered formations.

3.4. Morphological traits

3.4.1. SEM characterization of electrospun films

SEM characterization of keratin-based PLA films are demonstrated in Fig. 4 to highlight the morphological changes with keratin addition. At first sight, keratin containing cast film samples are visualized as uniform, yellow-colored and semi-transparent films. The surface of keratin film is smooth with no visible cracks or voids whereas PLA films are in more fragile nature. Electrospun film samples of both keratin and PLA are in white powder form. While keratin can easily form films, it is not possible to electrospin neat keratin. Therefore, literature examples employ a carrier polymer and/or polymeric blends for keratin electrospinning.

SEM image of Ker-F reveals entangled fiber formations with an average fiber diameter of 270 ± 27 nm. On the other hand, electrospun PLA-ES demonstrates sub-micron sized fibers with a wide fiber diameter distribution (596 ± 271 nm) where the fibers are relatively more aligned. Two distinct fiber size regions are observed in PLA-ES; one clustered in micron (908 ± 46 nm) and the other in sub-micron (408 ± 102 nm) region.

Evident from SEM images, PLA-F and KerPLA-F do not possess fiber properties, thus they are omitted from fiber size distribution graph (Fig. 4). SEM analysis of PLA-ES results in two distinct fiber size ranges, mainly arising from receded fiber jet takes place during electrospinning. Unlike Taylor cone, recessed jet is not stable and formation of this type of polymer jet results in wide range of fiber diameter [51]. Therefore, electrospun PLA-ES demonstrates some micron-sized fibers (1.02 ±

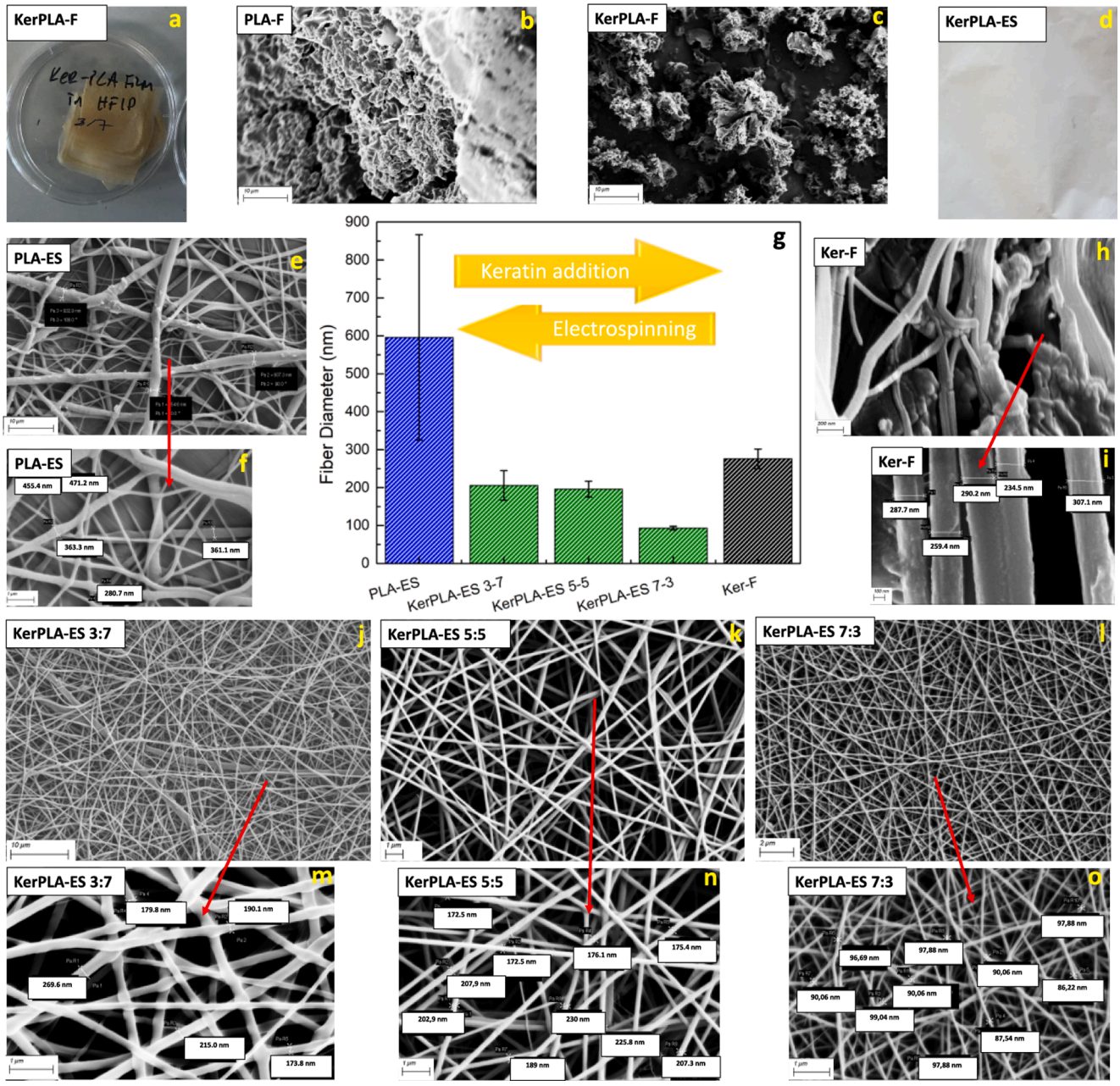

Fig. 4. Image of KerPLA-F (a), SEM images of PLA-F (b), KerPLA-F (c), image of KerPLA-ES (d), SEM images of PLA-ES at different magnifications (e, f), fiber size distribution of electrospun samples and keratin (g), SEM images of Ker-F at different magnifications (h, i), Ker-PLA-ES 3:7, 5:5, 7:3 (j, k, l) and their SEM morphologies at higher magnifications (m, n, o).

0.16 μm) along with submicron fibers (390 ± 77 nm).

SEM analysis of KerPLA-ES at different Ker/PLA ratio results in nanofibers with no evident bead formations. In addition, fiber diameters are observed to decrease with increasing keratin content. This can be attributed to decreased amorphous content around keratin fibers with PLA incorporation [52].

3.5. Thermomechanical properties

DMA analysis of keratin incorporated electrospun PLA films were investigated to observe the effect of keratin addition on storage modulii (E') and tan(δ) values of PLA. The onset of E' is related with long range molecular interactions (α relaxation) and provides crucial information on glass transition temperature (T_g). Evident from Fig. 5-a, all keratin incorporated electrospun PLA films possess single T_g as a result of miscible keratin PLA blends. There's a significant decrease in E' value of PLA below T_g due to constraints in segmental motions with nanofiber incorporation. Although keratin incorporation lowers storage modulus of PLA, 70 % keratin containing PLA (KerPLA-ES-7/3) exhibits the highest E' compared to other Ker-incorporated samples.

The drastic increase in tan(δ) observed in keratin incorporated films (Fig. 5-b) put forth a higher mobility in PLA chains with nanofiber addition. In contrast with E', the areas under tan(δ) curves of Ker-PLA samples do not follow a certain trend such as fiber ingredient. The multiple peaks observed between 90 and 130 °C represents cold crystallization [53]. Comparing DMA analyses Ker-incorporated electrospun PLA films KerPLA-ES-7/3 exhibits better E' and tan(δ).

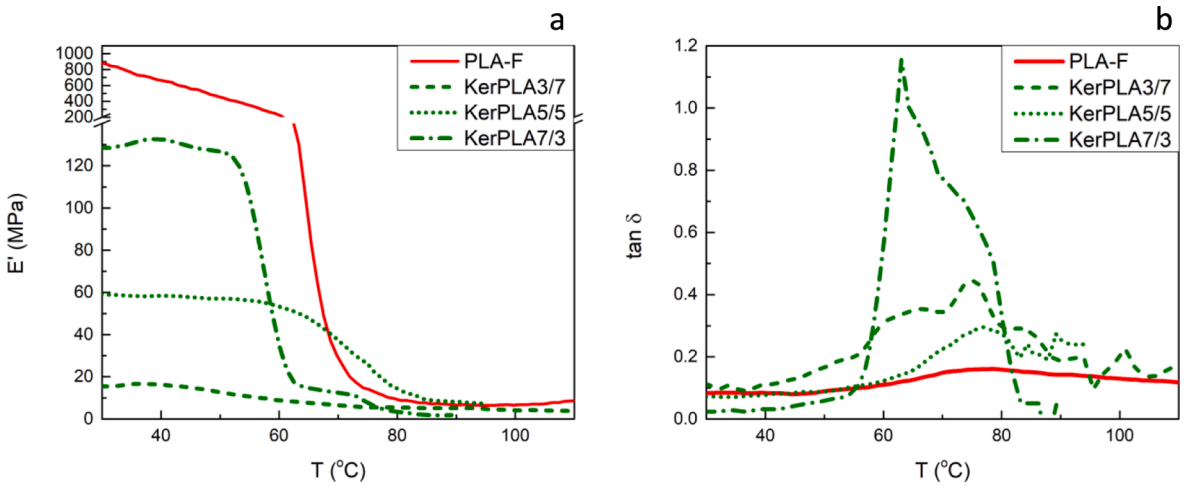

Fig. 5. DMA curves of electrospun PLA and Ker-PLA blend films in varying Keratin amount.

3.6. Antibacterial properties

Results of antibacterial activity tests performed against *S. aureus* ATCC 6538 and *Escherichia coli* ATCC 25922 were demonstrated in Table 2 and 3. Note that the ASTM E2149 standard test method was performed on Keratin film (Ker-F) as this sample is relatively brittle and could not be sized for JIS Z 2801 standard test method. Additionally, JIS Z 2801 method can measure the antibacterial activity of treated articles under static conditions. In contrast, ASTM E2149 method is used to determine the antimicrobial activity of materials under dynamic contact conditions. Table 4 shows results of ASTM E1249 test of Ker-F against *S. aureus* ATCC 6538 and E. *coli* ATCC 25922, respectively.

According to microbiological property tests, PLA-F and PLA-ES, similar reduction % and R values were obtained against the two tested bacteria. Same applies for Ker-F as its reduction % against *S. aureus* ATCC 6538 and E. *coli* ATCC 25922 resulted similar. Both samples preserved their antibacterial activity for 24 h. This means that both PLA and keratin are good packaging material candidates with wide spectrum of antibacterial activities. In addition to that, the presence of antibacterial activity in both PLA-F and PLA-ES samples imply that the PLA prepared by any method exhibits antibacterial activity.

All Ker-PLA electrospun films exhibit antibacterial activity against both Gram-positive and Gram-negative bacteria, independent of keratin content. Although KerPLA-3/7 exhibits strong antibacterial activity against *E. coli* (R = 7.53) with a reduction % > 99.9, it did not meet the criteria of R > 2 (R = 1.95) against *S. aureus* ATCC 6538 in JIS Z 2801 standard. Nonetheless, it still exhibits antibacterial activity against *E. coli* with a reduction % > 99.9. As the keratin content increases, electrospun films result with higher R values against *S. aureus* ATCC 6538. An R value > 2 is accounted as antibacterial, however, particularly for the Gram positive bacteria representative organisms, the R value is observed higher in the samples without keratin. Here, keratin may have a crucial role as a protective layer at static conditions, in dissociation of thick peptidoglycan layer present in Gram-positive bacteria. On the contrary, amount of keratin does not determine the antibacterial activity in Gram-negative evident from the R values observed in ASTM E2149 test of *E.coli* ATCC 6538. That being said, keratin film caused the same rate of death (> % 99.98 and > 3 log reduction) in both Gram-negative and Gram-positive bacteria under dynamic conditions (Table 4).

Table 2
Antibacterial activity results of Keratin included electrospun films against *S. aureus* ATCC 6538 after 24 h contact time according to JIS Z 2801 standard test method.

Sample	Microbial Load (cfu/cm^2)	Reduction%	R value
Control	2.0×10^5 (0 h) 1.85×10^8 (24 h)	–	–
PLA-F	7.5×10	> 99.9999	6.39
PLA-ES	8.5×10	> 99.9999	6.34
KerPLA-ES-3/7	2.07×10^6	98.88	1.95
KerPLA-ES-5/5	2.4×10^5	> 99.98	3.88
KerPLA-ES-7/3	2.81×10^3	> 99.998	4.82
Bacteria Control	2.00×10^5 (cfu/mL)		

Table 3
Antibacterial activity results of Keratin included electrospun films against *E.coli* ATCC 6538 after 24 h contact time according to JIS Z 2801 standard test method.

Sample	Microbial Load (cfu/cm^2)	Reduction%	R value
Control	4.0×105 (0. h) 3.44×10^8 (24 h)	–	–
PLA-F	<10*	> 99.99999	7.53
PLA-ES	<10	> 99.99999	7.53
KerPLA-ES-3/7	<10	> 99.9999	7.53
KerPLA-ES-5/5	4×10	99.9999	6.93
KerPLA-ES-7/3	<10	> 99.99999	7.53
Bacteria Control	4.1×10^5 (*kob/mL)		

* based on the average value. the detection limit of this test is 10 since the neutralizing agent is diluted by ×10.

Table 4
Antibacterial activity results of Ker-F acetic acid samples against *S. aureus* ATCC 6538 and E. *coli* ATCC 25922 after 24 h contact time according to ASTM E2149 standard test method.

***S. aureus* ATCC 6538**			
	Microbial Load (cfu/ml)		**Reduction %**
	0 h	**24 h**	**24 h**
Ker-F	–	3.15×10^4	99.98
Control	2.0×10^5	1.85×10^8	___
E. *coli* ATCC 25,922			
	Microbial Load (cfu/ml)		**Reduction %**
	0h	**24h**	**24h**
Ker-F	–	3.46×10^4	99.98
Control	4.1×10^5	3.44×10^8	___

3.7. Surface wettability

Water contact angle is a considerable approach to measure the moisture sensitivity of surfaces. The smaller contact angles (θ < 90)

formed between water drop and the surface are indicants of hydrophilicity, while larges values ($\theta > 90$) refer to hydrophobic surfaces. Comparing the water contact angles of electrospun and film surfaces of keratin-containing PLA samples, we observe a decreasing trend in hydrophilicity of PLA with respect to keratin incorporation and electrospinning. Electrospinning and keratin incorporation slightly reduces its hydrophobicity by 4.5 % and 7.2 %, respectively. These are expected as keratin is a considerably more hydrophilic material than PLA, and electrospinning process alters the surface charges of any material (Fig. 6). Evaluating the reduce in hydrophobic character of PLA by added amounts of keratin incorporation, we observe a decrease in contact angle value of PLA up to 21.2 % in the highest amount of keratin (KerPLA-ES 7/3). This is tolerable given the finding of increased antibacterial activity against *S. aureus* ATCC 6538 with increased keratin content. The bacterial cell wall of Gram-positive bacteria is more hydrophilic than Gram-negative with less lipid content in the cell wall (1–4 %). Incorporation of keratin provides a more hydrophilic environment to more easily interact with peptidoglycan layers present in Gram-positive bacteria and disrupt its cell wall. On the contrary, Gram-negative bacteria has a cell membrane containing lipopolysaccharide, which is hydrophobic to its nature, but is not directly associated with keratin content.

4. Conclusions

The current study explains the design, development, and performance evaluation of keratin-based electrospun antibacterial bioplastics.

Electrospinning parameters were optimized to produce the best aspect ratio in electrospun nanofibers. Electrospun fibers are observed in 30–70 wt% keratin containing samples using HFIP as solvent, with a flow rate of 0.1 mL/h, at 12 kV and 15 cm of collector distance. The wide range of keratin content provides varying nanofiber size in the electrospun films which enables the tuning of material properties. PLA is shown to alter crystallinity of keratin by introducing additional electrostatic interactions formed between keratin and PLA during electrospinning that dominates crystallinity, eventually making it more processable. The electrospinning process is observed to decrease the thermal stabilities of the biomaterials at hand. This is attributed to the constrained conformational relaxation of polymers with rapid solvent evaporation during electrospinning. During this rapid evaporation, keratin distorts the crystallization process of PLA resulting in imperfect crystals with lower thermal stabilities. Although thermal and thermomechanical properties of PLA lowers with nanofiber addition, 70 wt% keratin containing electrospun PLA films exhibits the ascendant thermal properties. Along with the thermal stability, the thermomechanical properties of PLA slightly lower with keratin addition and electrospinning. But again, the electrospun Ker-PLA films with the highest keratin content (70 wt% keratin) exhibits better thermomechanical performance and electrospinning with keratin provides tunable thermo-mechanics with respect to keratin content.

On the other hand, amount of keratin determines the antibacterial activity against Gram-positive bacteria whereas the activity against Gram-negative is independent of keratin content. Highest antibacterial activity in KerPLA-ES samples were obtained in KERPLA-ES-7/3 where the keratin content is the highest. Incorporation of keratin and electrospinning causes a 20 % loss in hydrophobicity of PLA. This is not a desired trait in a packaging material as hydrophobicity almost stands as a prerequisite for alternative plastics. Nevertheless, the antibacterial protection capacity of the developed electrospun films can be tuned against Gram-positive with the keratin content.

As a final insight, the present study proposes novel keratin incorporated electrospun bioplastics with tunable thermal, thermomechanical and antibacterial properties and recycled keratin-PLA electrospun films are a good candidate for food packaging applications. In 2020, the food packaging market size was estimated as $323.81 billion. With the global impact of COVID-19, packaging products witnessed a huge demand, raising their CAGR to 6.3 % in that year [54]. Biopolymer based packaging market is, on the other hand, expected to grow 12.6 % annually [55], doubling the CAGR of plastic packaging. In addition to replacing petroleum-based packaging products with natural alternatives, the development of renewable or recycled packaging technologies from biopolymers is also critical as 1.3 billions of food is estimated to be wasted every year [56].

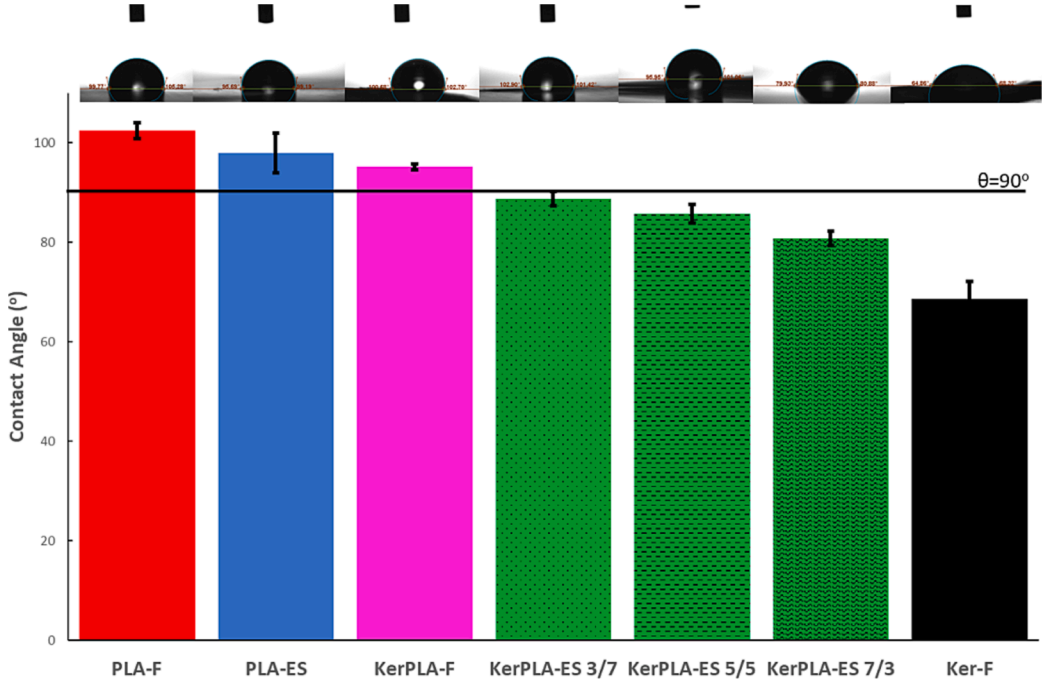

Fig. 6. Contact Angle values of Ker-PLA-ES surfaces obtained from contact angle measurements.

CRediT authorship contribution statement

Ayca Dicle Ertek: Writing – original draft. **Nazmiye Ozlem Sanli:** Writing – original draft, Writing – review & editing, Visualization. **Yusuf Ziya Menceloglu:** Writing – original draft, Conceptualization. **Senem Avaz Seven:** Writing – original draft, Writing – review & editing, Visualization, Conceptualization.

Declaration of Competing Interest

The authors declare that they have no known competing financial interests or personal relationships that could have appeared to influence the work reported in this paper.

Data availability

Data will be made available on request.

Acknowledgements

The authors would like to thank the EU funded KERAPACK project for their scientific contributions and efforts invested on the branding of bio-based packaging materials. The authors are aware that the end-user behavior is one of the most important driving forces behind the development of bio-based packaging industry and raising the awareness on sustainable packaging materials is crucial in these terms.

Funding

This project was funded by TUBITAK under the ManuNet EU project "KERAPACK: A novel integrated approach for the reduction, recycling and reuse of poultry feathers by keratins-based packaging manufacturing" (Reference Number: MNET17/NMAT-0060)

Appendix A. Supplementary material

Supplementary data to this article can be found online at https://doi.org/10.1016/j.eurpolymj.2022.111804.

References

[1] N. Eslahi, F. Dadashian, N.H. Nejad, An investigation on keratin extraction from wool and feather waste by enzymatic hydrolysis, Prep. Biochem. Biotechnol. 43 (7) (2013) 624–648.
[2] V. Agarwal, A.G. Panicker, S. Indrakumar, K. Chatterjee, Comparative study of keratin extraction from human hair, Int. J. Biol. Macromol. 133 (2019) 382–390.
[3] S. Alahyaribeik, A. Ullah, Methods of keratin extraction from poultry feathers and their effects on antioxidant activity of extracted keratin, Int. J. Biol. Macromol. 148 (2020) 449–456.
[4] M. Khumalo, B. Sithole, T. Tesfaye, Valorisation of waste chicken feathers: Optimisation of keratin extraction from waste chicken feathers by sodium bisulphite, sodium dodecyl sulphate and urea, J. Environ. Manage. 262 (2020), 110329.
[5] G.K.S. Arumugam, D. Sharma, R.M. Balakrishnan, J.B.P. Ettiyappan, Extraction, optimization and characterization of collagen from sole fish skin, Sustain. Chem. Pharm. 9 (2018) 19–26.
[6] M. Rajabi, A. Ali, M. McConnell, J. Cabral, Keratinous materials: Structures and functions in biomedical applications, Mater. Sci. Eng. C 110 (2020), 110612.
[7] J.H. Buchanan, A cystine-rich protein fraction from oxidized α-keratin, Biochem. J 167 (2) (1977) 489–491.
[8] K. Yamauchi, A. Yamauchi, T. Kusunoki, A. Kohda, Y. Konishi, Preparation of stable aqueous solution of keratins, and physiochemical and biodegradational properties of films, J. Biomed. Mater. Res.: Off. J. Soc. Biomater. Japn. Soc. Biomater. 31 (4) (1996) 439–444.
[9] H. Xie, S. Li, S. Zhang, Ionic liquids as novel solvents for the dissolution and blending of wool keratin fibers, Green Chem. 7 (8) (2005) 606–608.
[10] C. Tonin, M. Zoccola, A. Aluigi, A. Varesano, A. Montarsolo, C. Vineis, F. Zimbardi, Study on the conversion of wool keratin by steam explosion, Biomacromolecules 7 (12) (2006) 3499–3504.
[11] R.D.B. Fraser, T.P. MacRae, G.E. Rogers, Keratins: their composition, structure and biosynthesis, (1972).
[12] J. Navarro, J. Swayambunathan, M. Lerman, M. Santoro, J.P. Fisher, Development of keratin-based membranes for potential use in skin repair, Acta Biomater. 83 (2019) 177–188.
[13] S. Balaji, R. Kumar, R. Sripriya, P. Kakkar, D.V. Ramesh, P.N.K. Reddy, P.K. Sehgal, Preparation and comparative characterization of keratin–chitosan and keratin–gelatin composite scaffolds for tissue engineering applications, Mater. Sci. Eng. C 32 (4) (2012) 975–982.
[14] A. Tachibana, Y. Furuta, H. Takeshima, T. Tanabe, K. Yamauchi, Fabrication of wool keratin sponge scaffolds for long-term cell cultivation, J. Biotechnol. 93 (2) (2002) 165–170.
[15] J. Kirfel, T.M. Magin, J. Reichelt, Keratins: a structural scaffold with emerging functions, Cell. Mol. Life Sci. 60 (1) (2003) 56–71.
[16] S. Reichl, M. Borrelli, G. Geerling, Keratin films for ocular surface reconstruction, Biomaterials 32 (13) (2011) 3375–3386.
[17] Z. Shuihong, L. Wenhao, Z. Wenbin, L. Youhui, X.Y. Liu, Preparation of Free-standing Micropatterned Keratin Films by Soft Lithography, Acta Chim. Sin. 77 (6) (2019) 533–538.
[18] X. Mi, H. Xu, Y. Yang, Submicron amino acid particles reinforced 100% keratin biomedical films with enhanced wet properties via interfacial strengthening, Colloids Surf. B Biointerfaces 177 (2019) 33–40.
[19] S. Reakasame, D. Trapani, R. Detsch, A.R. Boccaccini, Cell laden alginate-keratin based composite microcapsules containing bioactive glass for tissue engineering applications, J. Mater. Sci. - Mater. Med. 29 (12) (2018) 185.
[20] G.M. Fortunato, F. Da Ros, S. Bisconti, A. De Acutis, F. Biagini, A. Lapomarda, C. Magliaro, C. De Maria, F. Montemurro, D. Bizzotto, Electrospun structures made of a hydrolyzed keratin-based biomaterial for development of in vitro tissue models, Front. Bioeng. Biotechnol. 7 (2019) 174.
[21] D.O.S. Ramirez, R.A. Carletto, C. Tonetti, F.T. Giachet, A. Varesano, C. Vineis, Wool keratin film plasticized by citric acid for food packaging, Food Packag. Shelf Life 12 (2017) 100–106.
[22] I. Sinkiewicz, A. Śliwińska, H. Staroszczyk, I. Kołodziejska, Alternative methods of preparation of soluble keratin from chicken feathers, Waste Biomass Valoriz. 8 (4) (2017) 1043–1048.
[23] P. Pardo-Ibáñez, A. Lopez-Rubio, M. Martínez-Sanz, L. Cabedo, J.M. Lagaron, Keratin–polyhydroxyalkanoate melt-compounded composites with improved barrier properties of interest in food packaging applications, J. Appl. Polym. Sci. 131 (4) (2014).
[24] G.S. Cao, Z.P. Zhang, M.Z. Rong, M.Q. Zhang, A novel strategy for producing high-performance continuous regenerated fibers with wool-like structure, SusMat 2 (1) (2022) 90–103.
[25] C. Tonin, A. Aluigi, A. Varesano, C. Vineis, Keratin-based nanofibres, nanofibers, INTECH (2010) 139–158.
[26] E.D. Boland, J.A. Matthews, K.J. Pawlowski, D.G. Simpson, G.E. Wnek, G. L. Bowlin, Electrospinning collagen and elastin: preliminary vascular tissue engineering, Front. Biosci. 9 (2) (2004) 1422–1432.
[27] A. Aluigi, C. Vineis, A. Varesano, G. Mazzuchetti, F. Ferrero, C. Tonin, Structure and properties of keratin/PEO blend nanofibres, Eur. Polym. J. 44 (8) (2008) 2465–2475.
[28] E. Klimov, V. Raman, R. Venkatesh, W. Heckmann, R. Stark, Designing nanofibers via electrospinning from aqueous colloidal dispersions: effect of cross-linking and template polymer, Macromolecules 43 (14) (2010) 6152–6155.
[29] J. Li, Y. Li, L. Li, A.F.T. Mak, F. Ko, L. Qin, Preparation and biodegradation of electrospun PLLA/keratin nonwoven fibrous membrane, Polym. Degrad. Stab. 94 (10) (2009) 1800–1807.
[30] S. Goyal, M. Dotter, E. Diestelhorst, J.L. Storck, A. Ehrmann, B. Mahltig, Extraction of keratin from wool and its use as biopolymer in film formation and in electrospinning for composite material processing, J. Eng. Fibers Fabrics 17 (2022) 15589250221090499.
[31] M.T. Islam, R.M. Laing, C.A. Wilson, M. McConnell, M.A. Ali, Fabrication and characterization of 3-dimensional electrospun poly (vinyl alcohol)/keratin/chitosan nanofibrous scaffold, Carbohydr. Polym. 275 (2022), 118682.
[32] D.H. Baek, C.S. Ki, I.C. Um, Y.H. Park, Metal ion adsorbability of electrospun wool keratose/silk fibroin blend nanofiber mats, Fibers Polym. 8 (3) (2007) 271–277.
[33] R. Auras, B. Harte, S. Selke, An overview of polylactides as packaging materials, Macromol. Biosci. 4 (9) (2004) 835–864.
[34] I. Armentano, N. Bitinis, E. Fortunati, S. Mattioli, N. Rescignano, R. Verdejo, M. A. López-Manchado, J.M. Kenny, Multifunctional nanostructured PLA materials for packaging and tissue engineering, Prog. Polym. Sci. 38 (10–11) (2013) 1720–1747.
[35] F.K. Mwiiri, R. Daniels, Influence of PVA Molecular Weight and Concentration on Electrospinnability of Birch Bark Extract-Loaded Nanofibrous Scaffolds Intended for Enhanced Wound Healing, Molecules 25 (20) (2020) 4799.
[36] A.L. Yarin, S. Koombhongse, D.H. Reneker, Taylor cone and jetting from liquid droplets in electrospinning of nanofibers, J. Appl. Phys. 90 (9) (2001) 4836–4846.
[37] M. Zoccola, A. Aluigi, C. Vineis, C. Tonin, F. Ferrero, M.G. Piacentino, Study on cast membranes and electrospun nanofibers made from keratin/fibroin blends, Biomacromolecules 9 (10) (2008) 2819–2825.
[38] D.M. Byler, H. Susi, Examination of the secondary structure of proteins by deconvolved FTIR spectra, Biopolymers, Orig. Res. Biomol. 25 (3) (1986) 469–487.
[39] H.H. Mantsch, D. Chapman, Infrared spectroscopy of biomolecules, Wiley-Liss New York, 1996.
[40] Y.i. Menceloğlu, Y.Z. Menceloğlu, S.A. Seven, Triblock Superabsorbent Polymer Nanocomposites with Enhanced Water Retention Capacities and Rheological Characteristics, ACS Omega (2022).
[41] S.R. Ryu, I. Noda, Y.M. Jung, Positional fluctuation of IR absorption peaks: Frequency shift of a single band or relative intensity changes of overlapped bands, Am. Lab. 43 (4) (2011) 40–43.

[42] K.T. Yilma, T. Tesfaye, H. Enawgaw, M. Ayele, D.Y. Limeneh, M. Gibril, F. Kong, Optimizing the Extraction of Keratin from Cattle Hoof Using Central Composite Design, Adv. Mater. Sci. Eng. 2022 (2022).
[43] B.Y. Alashwal, M.S. Bala, A. Gupta, S. Sharma, P. Mishra, Improved properties of keratin-based bioplastic film blended with microcrystalline cellulose: A comparative analysis, Journal of King Saud University-Science 32 (1) (2020) 853–857.
[44] S. Li, X.-H. Yang, Fabrication and characterization of electrospun wool keratin/poly (vinyl alcohol) blend nanofibers, Adv. Mater. Sci. Eng. 2014 (2014).
[45] W. Du, L. Zhang, C. Zhang, J. Cao, D. Wang, H. Li, W. Li, J. Zeng, Green and Highly Efficient Wool Keratin Extraction by Microwave Induction Method, (2022).
[46] M. Spei, R. Holzem, Further thermoanalytical investigations of annealed keratins: The time and temperature dependence, Colloid Polym. Sci. 268 (7) (1990) 630–635.
[47] J. Cao, F. Leroy, Depression of the melting temperature by moisture for α-form crystallites in human hair keratin, Biopolymers, Orig. Res. Biomol. 77 (1) (2005) 38–43.
[48] M. Spei, R. Holzem, Thermoanalytical investigations of extended and annealed keratins, Colloid Polym. Sci. 265 (11) (1987) 965–970.
[49] Ç. Girişken, S.A. Seven, O.G. Ersoy, Y.Z. Menceloğlu, Investigation of structure-morphology-function relationship of plastomers used to produce low mold shrinkage thermoplastic olefins, Eur. Polym. J. 159 (2021), 110758.
[50] K. Kadirvelu, N.N. Fathima, Self-assembly of keratin peptides: Its implication on the performance of electrospun PVA nanofibers, Sci. Rep. 6 (2016) 36558.
[51] S. Zargham, S. Bazgir, A. Tavakoli, A.S. Rashidi, R. Damerchely, The effect of flow rate on morphology and deposition area of electrospun nylon 6 nanofiber, J. Eng. Fibers Fabrics 7(4) (2012) 155892501200700414.
[52] Y. Yu, W. Yang, M.A. Meyers, Viscoelastic properties of α-keratin fibers in hair, Acta Biomater. 64 (2017) 15–28.
[53] J. Moczo, D. Kun, E. Fekete, Desiccant effect of starch in polylactic acid composites, Express Polym. Lett. 12 (2018) 1014–1024.
[54] L. Motelica, D. Ficai, A. Ficai, O.C. Oprea, D.A. Kaya, E. Andronescu, Biodegradable antimicrobial food packaging: Trends and perspectives, Foods 9 (10) (2020) 1438.
[55] C. Popa, Private equity challenge-Kompuestos as an investment opportunity in the plastic industry, (2021).
[56] R. Ishangulyyev, S. Kim, S.H. Lee, Understanding food loss and waste—why are we losing and wasting food? Foods 8 (8) (2019) 297.